X-651-73-57

PREPRINT

NASA TM X- 66190

A COMPOSITE STUDY OF CLOUD, OZONE AND OTHER DATA FROM RECENT SATELLITE EXPERIMENTS

M. S. V. RAO
A. J. KRUEGER
C. PRABHAKARA

FEBRUARY 1973

GSFC — GODDARD SPACE FLIGHT CENTER —
GREENBELT, MARYLAND

X-651-73-57

A COMPOSITE STUDY OF CLOUD, OZONE AND OTHER DATA FROM RECENT SATELLITE EXPERIMENTS

M. S. V. Rao
A. J. Krueger
and
C. Prabhakara

February 1973

GODDARD SPACE FLIGHT CENTER
Greenbelt, Maryland

CONTENTS

ILLUSTRATIONS

ILLUSTRATIONS (Continued)

ILLUSTRATIONS (Continued)

TABLES

A COMPOSITE STUDY OF CLOUD, OZONE AND OTHER DATA FROM RECENT SATELLITE EXPERIMENTS

M. S. V. Rao
A. J. Krueger
and
C. Prabhakara

ABSTRACT

Pictorial data from the Image Dissector Camera System (IDCS) and Temperature-Humidity Infrared Radiometer (THIR) experiments on Nimbus 4 satellite are analyzed along with (a) global total ozone maps prepared from Infrared Interferometer Spectrometer (IRIS) data and (b) total ozone and its vertical distribution as derived from Backscatter Ultraviolet (BUV) spectrometer data. A close relationship is generally observed between centers of high ozone and vortices in the IDCS and THIR montages. This is also confirmed by low centers in the 200 mb Northern Hemisphere charts. The vertical distribution of ozone indicates that the enhancement in ozone in these cases occurs in the lower stratosphere (and possibly to a minor extent in the troposphere) rather than in the upper stratosphere and mesosphere.

In the tropical belt, a longitudinal inhomogeneity is noticed in cloudiness as well as ozone distribution, in that there is consistently less cloud cover and somewhat higher ozone in the African and adjoining Indian Ocean regions than over the rest of the belt, with corresponding non-uniformity in sea-surface

temperature. A possible atmospheric circulation pattern consistent with this distribution (involving a reversed Hadley cell locally over the Indo-African region in summer) is considered.

The relation between ozone gradients and jet streams observed in earlier work, is further substantiated.

1. INTRODUCTION

Recent satellite experiments have provided a wealth of meteorological data on a global scale (especially over inaccessible areas) of which a considerable portion remain to be analyzed. In this paper are presented the results of a composite study of some of the data from a number of such experiments (mainly those on Nimbus 3 and 4 satellites). The data analyzed are listed in Table 1.

IDCS (Werner and Branchflower 1970) and THIR (McCulloch 1970) pictorial data were analyzed along with daily global total ozone maps prepared from IRIS (Hanel, Conrath and Schlachman 1970) data and total ozone and its vertical distribution derived from available BUV spectrometer (Heath, Krueger and Mateer 1970) data, as well as with 200 mb Northern Hemisphere charts of the Numerical Weather Prediction Unit of NOAA. The distribution of average cloudiness presented in the "Global Atlas of Relative Cloud Cover 1967-70" were studied along with similar mean charts of ozone amount, as well as with average sea-surface temperature charts derived from Nimbus 4 THIR data. The period of study is chiefly 15th of April through 15th June 1970 (although a few cases falling outside this period when good data from the different experiments were available have also been examined).

Table 1

(Data Sources)

Information	Source
1. Image Dissector Camera System pictorial data	Nimbus 4 Data Catalog
2. Temperature-Humidity Infrared Radiometer pictorial data	Nimbus 4 Data Catalog
3. Infrared Interferometer Spectrometer data of total ozone	C. Prabhakara
4. Backscatter Ultraviolet Spectrometer data of total ozone and its vertical distribution	D. Heath A. J. Krueger
5. 200 mb Northern Hemispheric charts	NWP Unit of NOAA
6. Global Cloud Cover 1967-70	U.S. Department of Commerce and the USAF
7. Sea-surface temperature chart from THIR data	V. V. Salomonson

2. TROPOSPHERIC VORTICES AND OZONE

The intercomparison of daily data brought out a great many cases in which there is a close relationship between vortices in the IDCS and THIR montages and centers of high ozone inferred from IRIS and BUV data. Forty-two such cases were observed during the period under study. These are listed in Table 2. A few representative cases are illustrated in Figures 1 to 4.

Table 2

Vortex and Ozone Centers

(a) Northern Hemisphere

	Date	Orbit #	IDCS Vortex Center		THIR Vortex Center		IRIS Ozone High		200 mb Low Center	
1	April 20	165	45N	54W	45N	54W	46N	57W	45N	55W
2	April 24	224	48N	162E	48N	162E	46N	160E	48N	160E
3	April 28	270	63N	7E	63N	7E	60N	7E	65N	5E
4	May 8	405	46N	10W	46N	10W	48N	10W	45N	12W
5	May 8	407	49N	63W	49N	63W	49N	63W	47N	65W
6	May 18	540	54N	30W	24N	30W	54N	32W	55N	32W
7	May 19	554	39N	35W	39N	35W	38N	37W	38N	35W
8	May 20	567	38N	37W	38N	37W	38N	37W	38N	37W
9	May 21	579	38N	17E	38N	17E	40N	15E	39N	16E
10	May 21	580/1	41N	31W	41N	31W	40N	30W	41N	34W
11	May 22	587/8	52N	128E	52N	128E	50N	127E	50N	132E
12	May 25	627	51N	166E	51N	166E	49N	168E	49N	169E

Table 2 Continued

	Date	Orbit #	IDCS Vortex Center		THIR Vortex Center		IRIS Ozone High		200 mb Low Center	
13	May 26	648	62N	50W	62N	50W	61N	52W	61N	51W
14	May 27	660/1	67N	30W	67N	30W	63N	33W	63N	30W
15	May 30	702	64N	42W	64N	42W	60N	46W	64N	45W
16	June 2	743	33N	63W	33N	63W	33N	66W	31N	64W
17	June 3	761	48N	160E	48N	160E	50N	156E	50N	156E
18	June 4	771	34N	95W	34N	95W	37N	95W	36N	95W
19	June 5	782	58N	46W	58N	46W	61N	47W	60N	50W
20	June 5	788	53N	162E	53N	162E	57N	168W	55N	160W
21	June 9	835	40N	23W	40N	23W	44N	20W	44N	20W
22	June 11	856	55N	135E	55N	135E	59N	125E	57N	130E
23	June 11	862	48N	17W	48N	17W	50N	15W	48N	15W
(b) Southern Hemisphere										
24	April 21	180	45S	130E	45S	130E	40S	130E		
25	April 28	266	61S	160E	61S	160E	58S	155E		
26	April 30	292	38S	169E	38S	169E	41S	170E		
27	April 30	296	49S	65E	49S	65E	49S	65E		
28	April 30	299	51S	19W	51S	19W	50S	20W		
29	May 18	540	53S	30W	53S	30W	54S	52W		
30	May 19	550	53S	84E	53S	84E	48S	78E		
31	May 20	564	46S	85E	46S	85E	45S	83E		

Table 2 Continued

	Date	Orbit #	IDCS Vortex Center		THIR Vortex Center		IRIS Ozone High		200 mb Low Center
32	May 23	604	50S	89E	50S	89E	50S	87E	
33	May 23	610	54S	89W	54S	89W	55S	85W	
34	May 25	635	43S	33W	44S	33W	40S	30W	
35	June 5	782	55S	1W	55S	1W	51S	0	
36	June 8	819	54S	85E	54S	85E	53S	82E	
37	June 8	821	47S	26E	47S	26E	46S	25E	
38	June 8	825	45S	79W	45S	79W	44S	76W	
39	June 9	832	48S	98E	48S	98E	45S	102E	
40	June 14	899	53S	94E	53S	94E	53S	96E	
41	June 14	906	50S	86W	50S	86W	46S	87W	
42	June 15	912	50S	109E	50S	109E	53S	114E	

1. A vortex centered at 48N 162E may be seen in the imagery obtained during Nimbus 4 orbit 224 on April 24, 1970 by IDCS (Figure 1a) and by THIR (Figure 2a). The IRIS ozone map for April 24 (Figure 1c) shows a high centered nearly at 46N 160E. The corresponding 200 mb chart (Figure 1d) shows up a low around 48N 160E.

2. Figures 2a, b, and c relate to a vortex in the Southern Hemisphere on April 30.

3. Figures 3a, b, c, and d illustrate a situation on May 20.

←------- Figure 1a. Vortex of April 24, 1970 as observed by IDCS, orbit 224

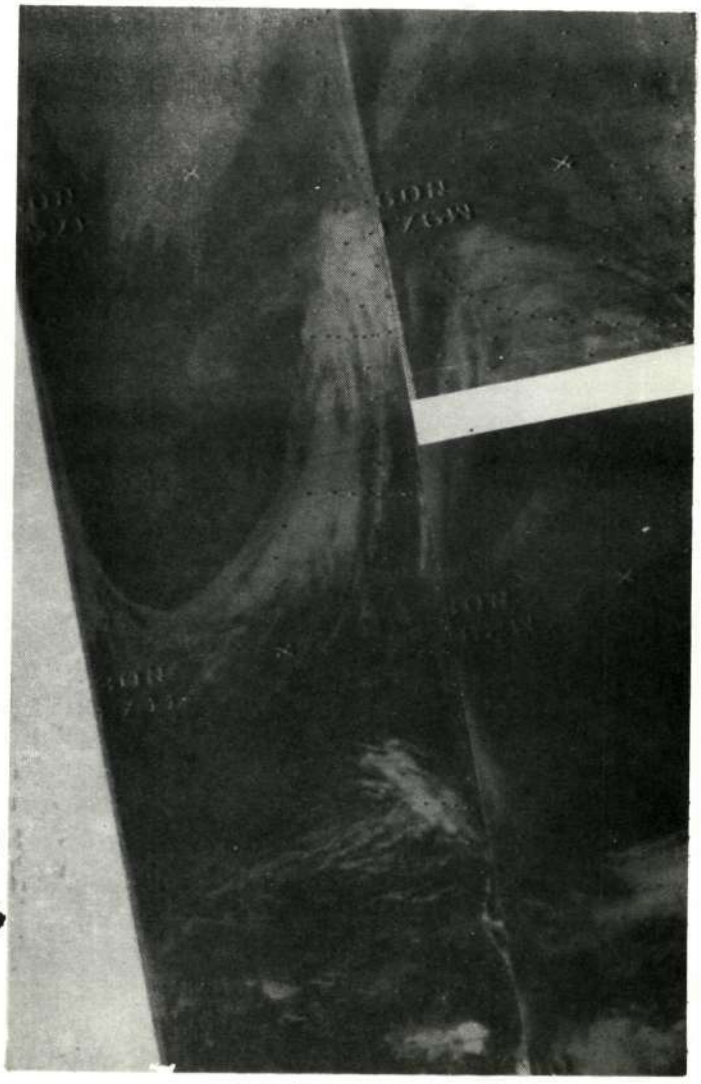

Figure 1b. The same vortex as observed by THIR (11.5μ) orbit 224 ------->

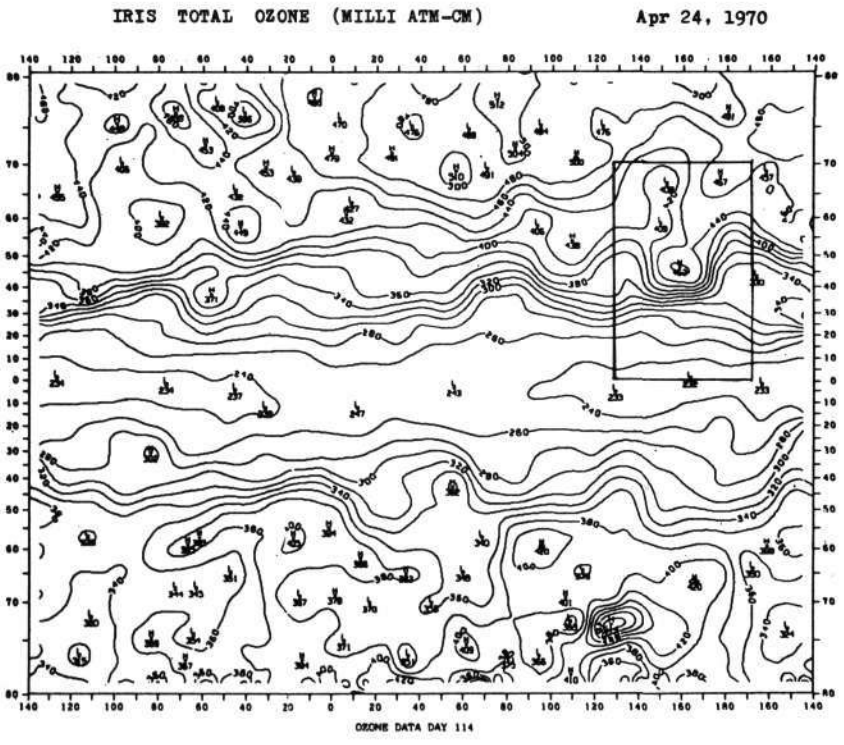

Figure 1c. IRIS total ozone map of April 24, 1970

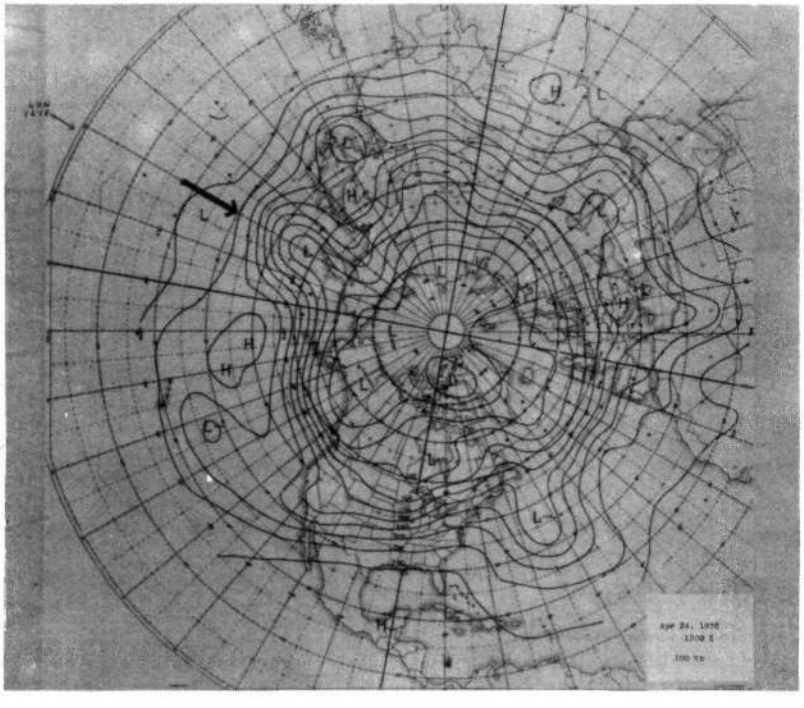

Figure 1d. 200 mb chart of the same day

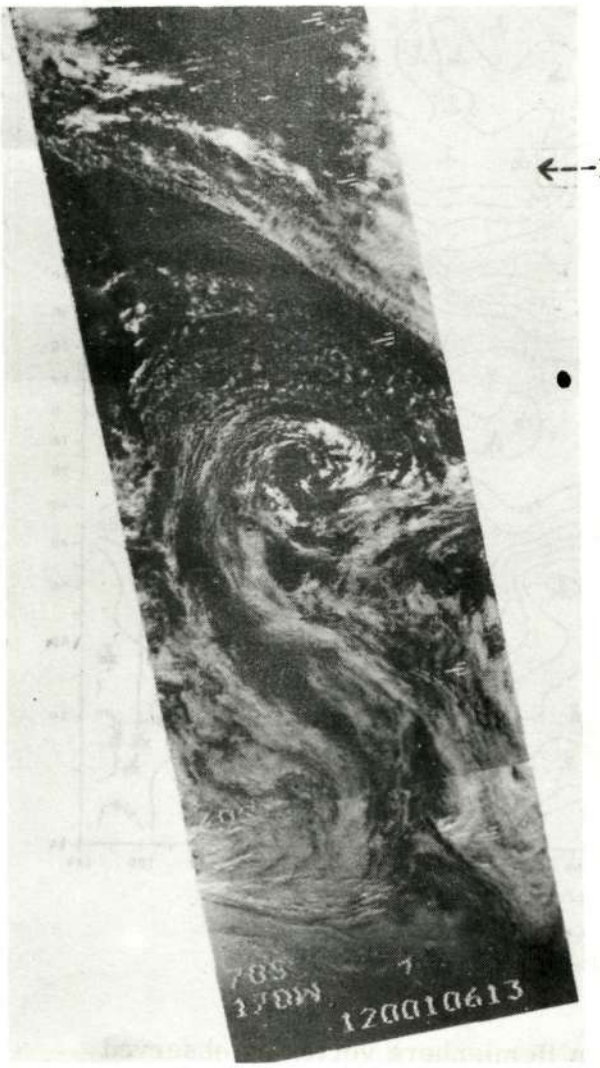

←--Figure 2a. Southern Hemisphere vortex of April 30, 1970 as observed by IDCS orbit 292

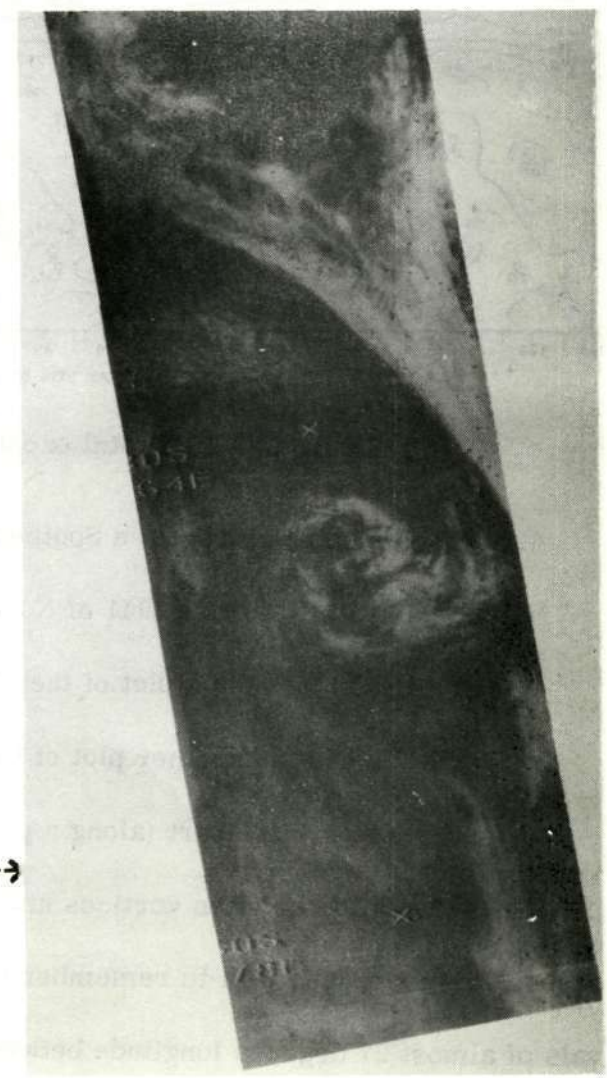

Figure 2b. The same vortex as observed by THIR (11.5μ) orbit 292 --------→

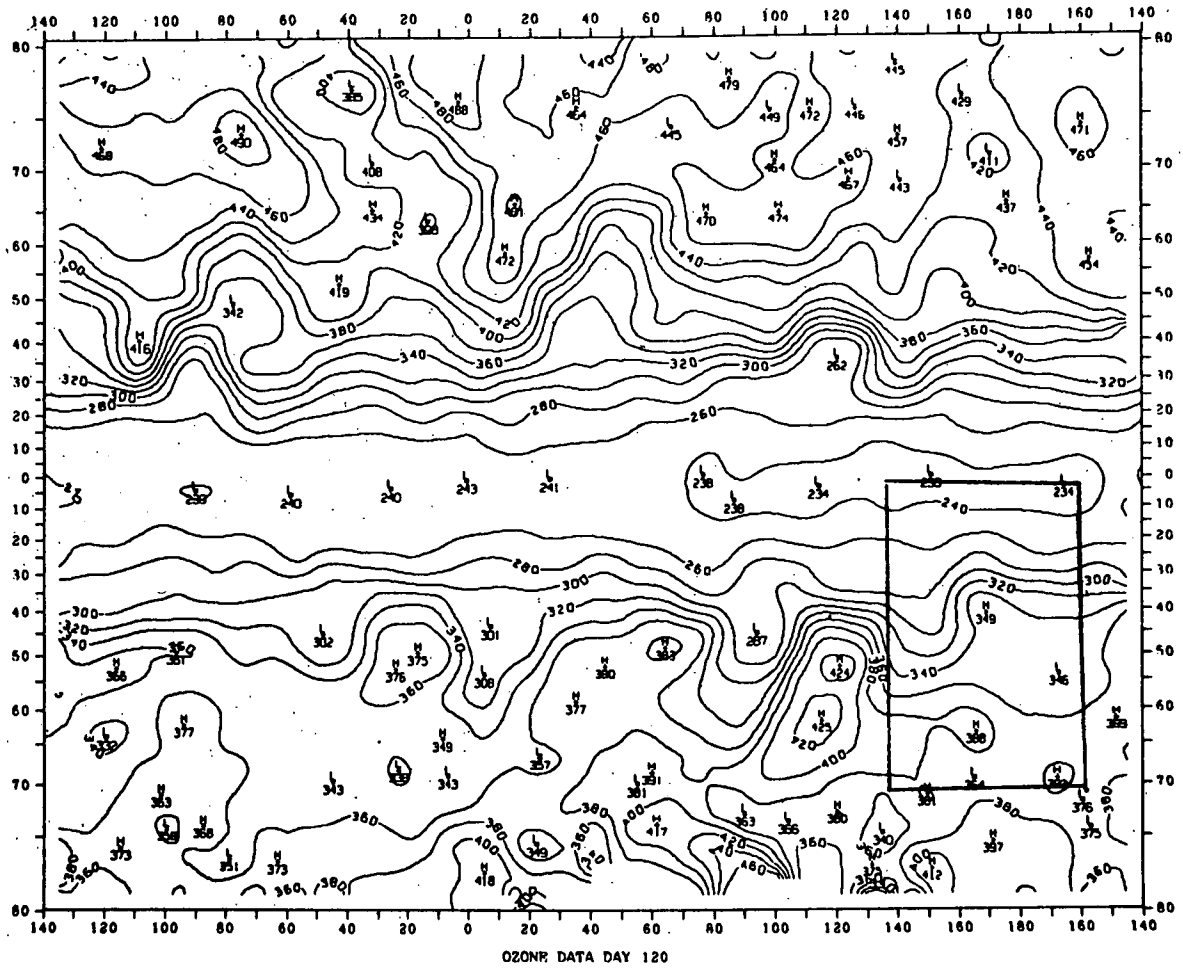

Figure 2c. IRIS total ozone map of April 30, 1970

4. Figures 4a and b reveal a Southern Hemisphere vortex as observed during satellite orbit 2941 of November 13, by IDCS and THIR. In Figure 4c can be seen a plot of the BUV total ozone data during the same orbit as well as another plot of total ozone obtained during the scan a couple of orbits apart (along a path which is clear of the vortex).

The association between vortices and ozone maxima is evident in the above cases. However, it is well to remember that ozone data are obtained at intervals of almost 27 degrees longitude between successive orbits, and even with

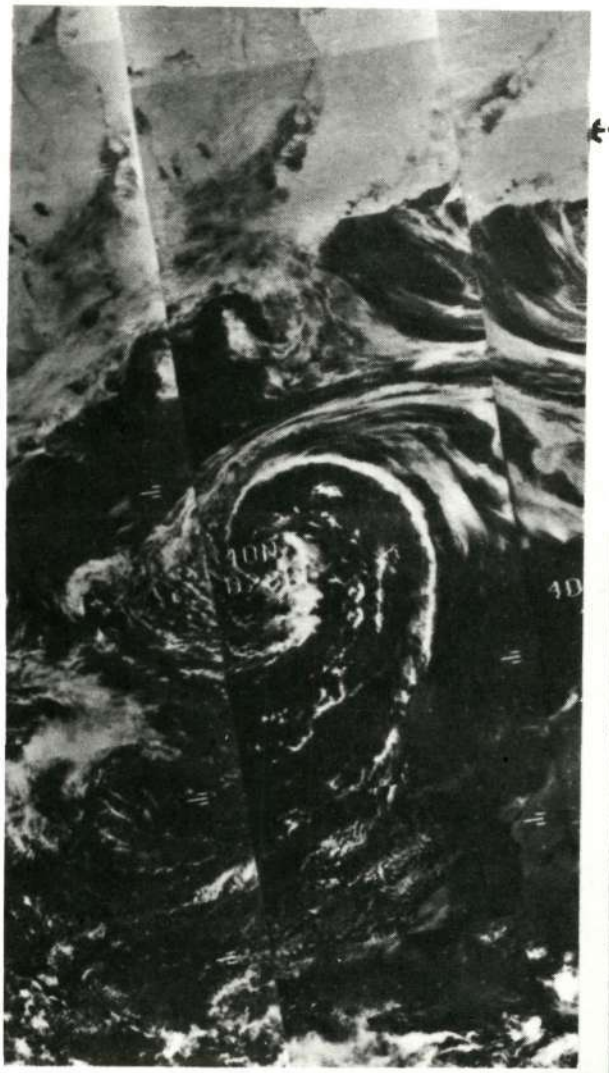

←Figure 3a. Vortex of May 20, 1970 as observed by IDCS orbit 567

Figure 3b. The same vortex as observed by THIR (11.5μ) orbit 567 ---------→

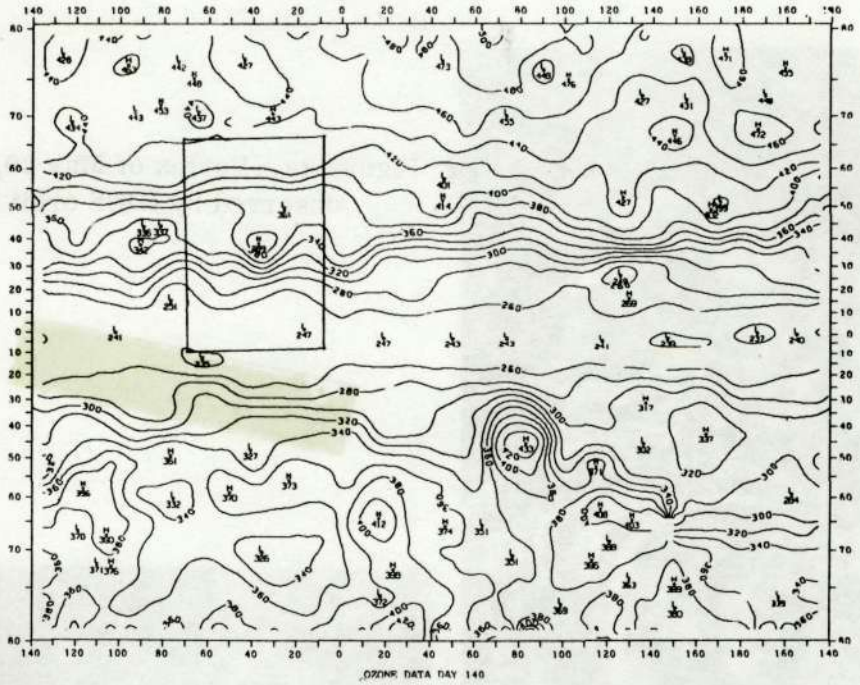

Figure 3c. IRIS total ozone map of May 20, 1970

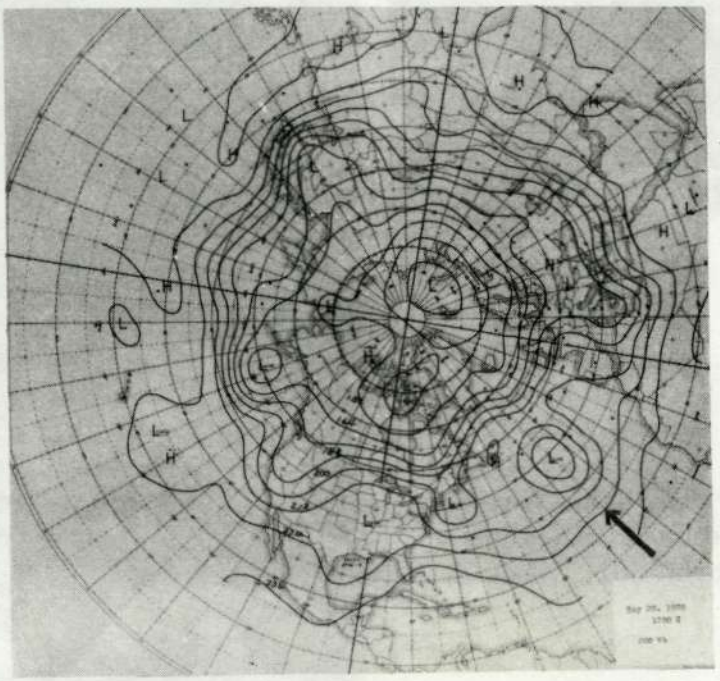

Figure 3d. 200 mb chart of the same day

←Figure 4a. Southern Hemisphere vortex of Nov. 13, 1970 as observed by IDCS orbit 2940/1

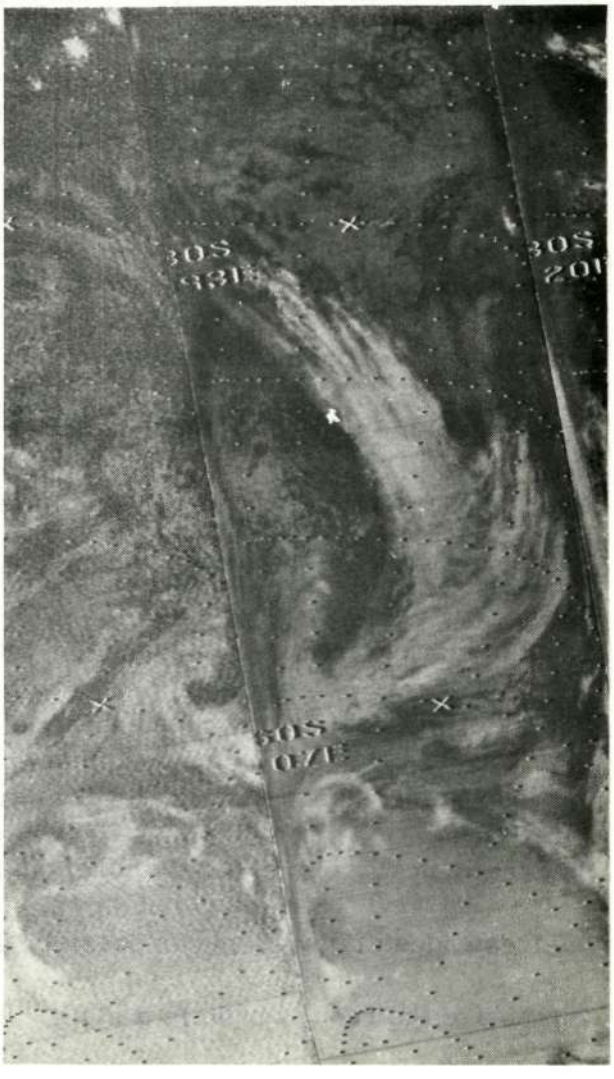

Figure 4b. The same vortex as observed by THIR (11.5 μ) orbit 2940/1 ---------→

nighttime IRIS observations, the average longitudinal separation of data on any single day exceeds 13 degrees; hence, although the centers of maxima have been determined objectively by a computer technique employing a polynomial fit for observed gradients, there is an inherent uncertainty in their location. Owing to this and other imperfections in the data, and the unavailability of information simultaneously from all the experiments on many occasions for composite study, it is not possible to establish a one to one correspondence between vortex centers and ozone maxima. Yet, the data are sufficient to point towards a strong relationship.

The BUV experiment provides a means of examining on these occasions, at what level the main changes in ozone occur. Figure 4d represents the integrated ozone amounts above the pressure surfaces 20 mb and 10 mb associated with the total ozone measurements presented in Figure 4c. A comparison of the two figures reveals that while the enhancement in total ozone is about 100 milli-atmosphere-centimeters (or Dobson units), the change is reduced to 10 Dobson units above 20 mb, and becomes negligible above 10 mb. Again in Figure 5a a similar marked increase in ozone may be noted at latitude 69S along the scan path of orbit 2934, as compared with the observations during orbit 2936. The corresponding changes at high level as seen in Figure 5b, are small above 20 mb and really negligible above 10 mb. No doubt, it is better to study ozone maps over extended areas whenever possible instead of individual orbits. Figures 6a and 6b are the results of such a study. In the total ozone map of the Southern

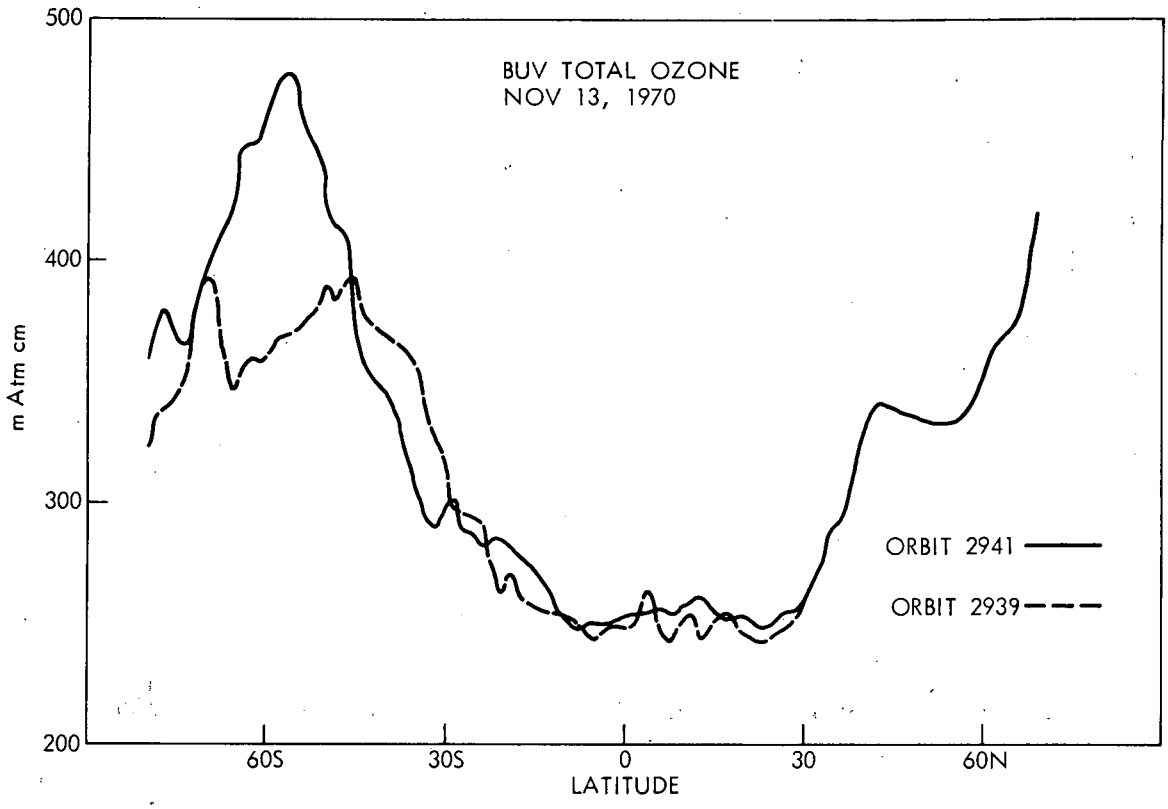

Figure 4c. BUV total ozone data obtained during orbits 2941 and 2939

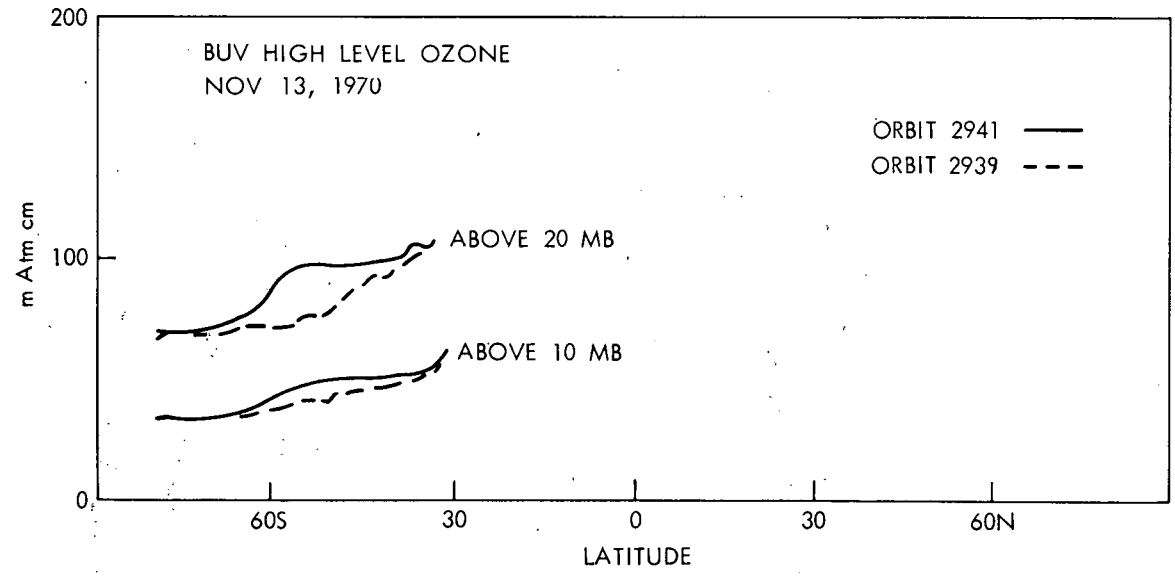

Figure 4d. Integrated ozone amounts above 20 mb and 10 mb corresponding to the total ozone data in Figure 4c

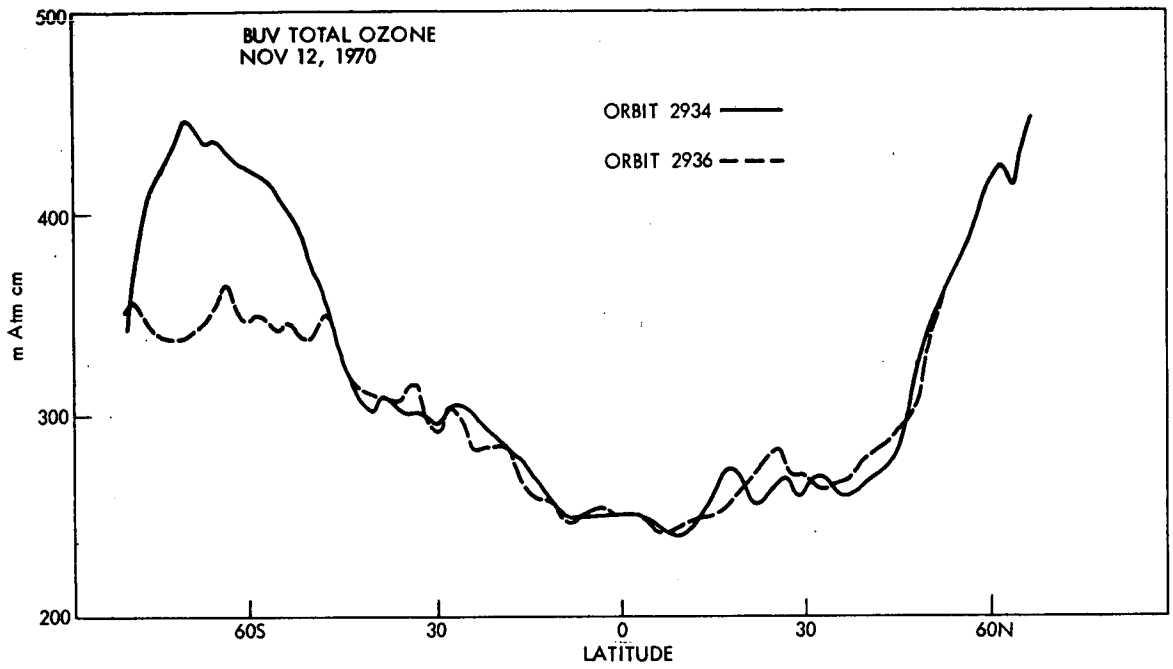

Figure 5a. BUV total ozone data obtained during orbits 2934 and 2936

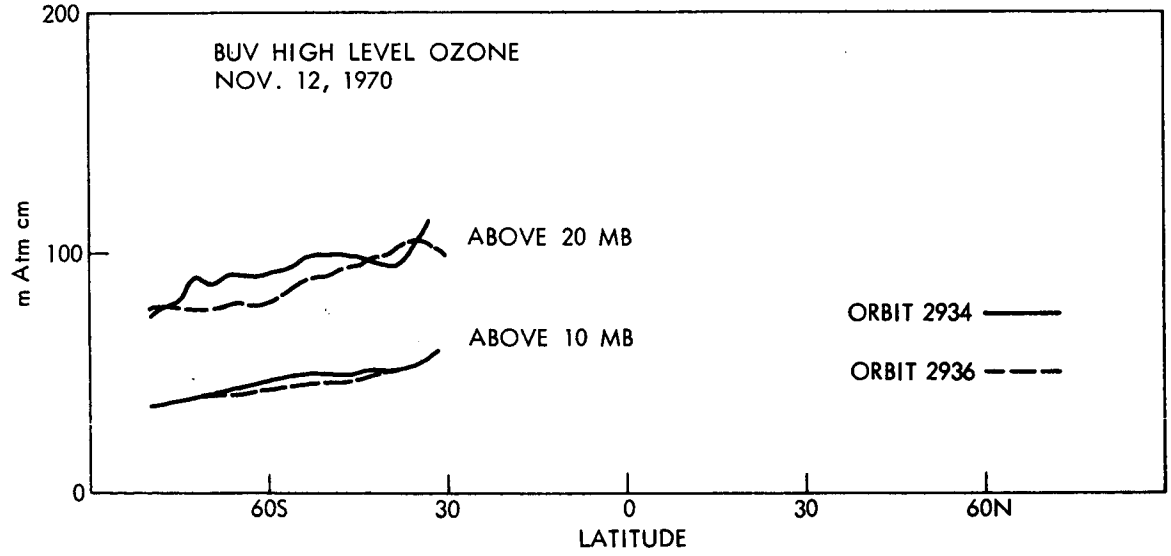

Figure 5b. Integrated ozone amounts above 20 mb and 10 mb observed during the same orbits

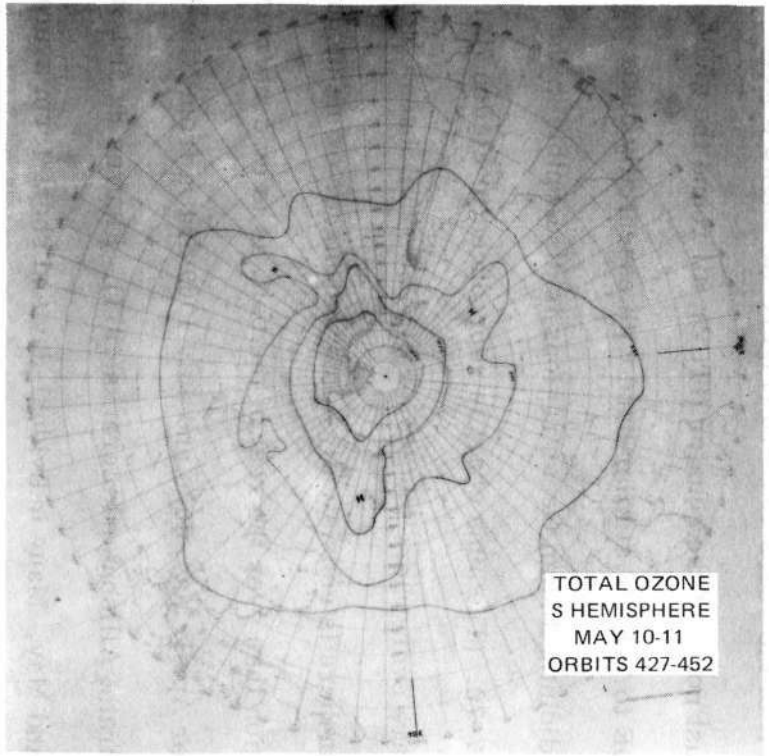

Figure 6a. Total ozone chart for the Southern Hemisphere May 10-11

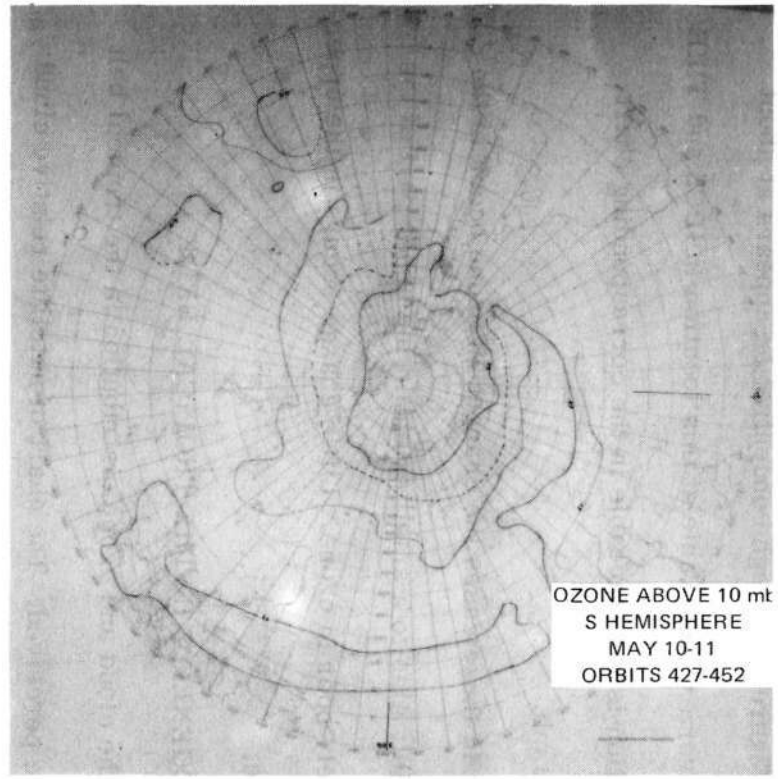

Figure 6b. Chart of ozone above 10 mb for the Southern Hemisphere May 10-11

Hemisphere for May 10-11 (Figure 6a) a high concentration appears at about 47S 100E corresponding to a vortex observable at this location in IDCS and THIR imagery; this high concentration is not traceable in the corresponding chart (Figure 6b) of ozone above 10 mb.

It would thus appear that in these cases the changes in ozone occur in the lower stratosphere and possibly also to a small extent in the upper part of the troposphere which is relatively poor in ozone. Little change occurs in the upper stratosphere and mesosphere.

3. LONGITUDINAL INHOMOGENEITY IN THE TROPICAL BELT

On looking carefully at the cloud and ozone distribution in the tropical belt, an interesting feature may be perceived. The chart of satellite relative cloud cover in mean octas, for April of the years 1967-70 (Figure 7a) shows a well-marked band of cloudiness just north of the equator (ITCZ), all round the globe except between longitudes 30E to 70E. A similar band with essentially clear skies over the African and adjoining Indian Ocean regions is discernible in the charts for May and June 1967-70. (The June chart is reproduced in Figure 7b.) Ozone values in the tropics are everywhere low, generally 250 ±25 Dobson units. But within the equatorial belt there is consistently somewhat higher ozone (about 10%) in the Indo-African region than over the rest of the belt, as is evident from mean monthly ozone maps for April, May, June and July 1969 drawn from Nimbus 3 data (Prabhakara, Conrath, Allison and Steranka 1971). Figures 8a and 8b display the maps for April and May. Many individual-day and short-term average

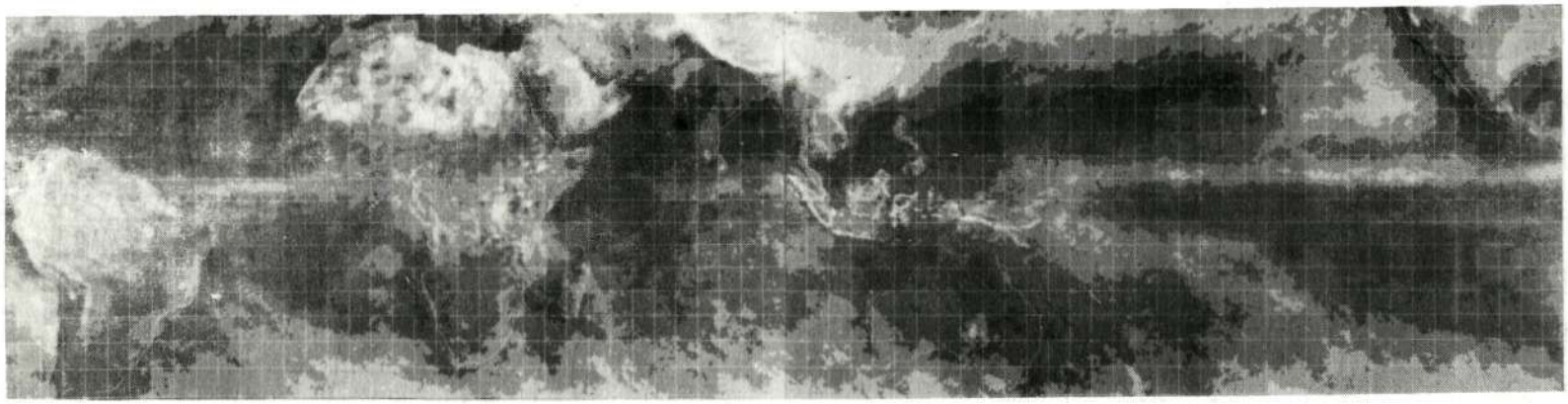

Figure 7a. Satellite cloud cover (mean octas) April 1967-70

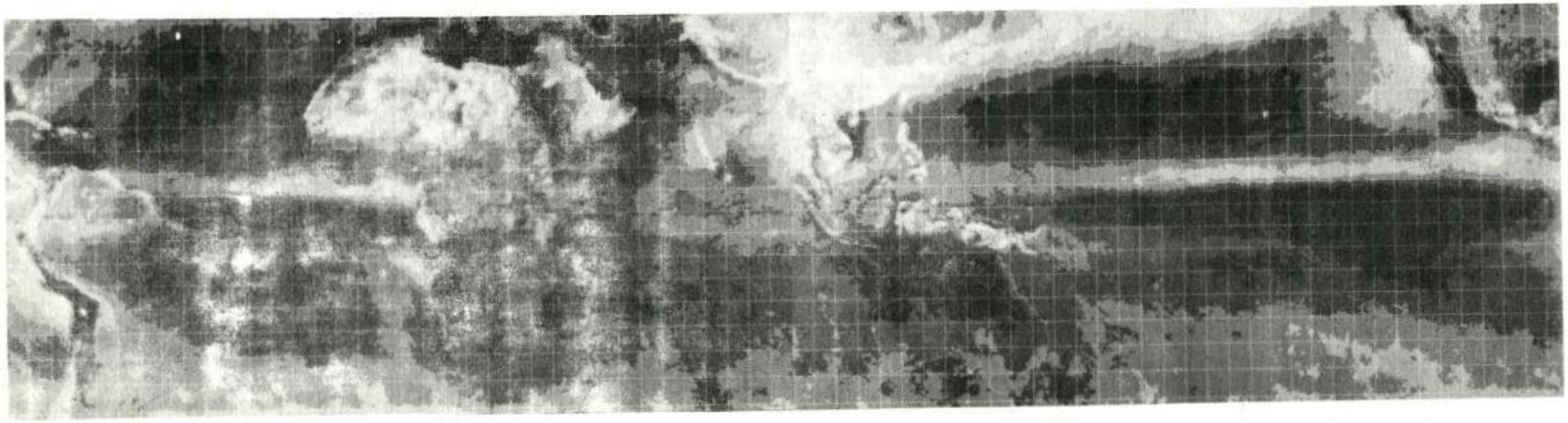

Figure 7b. Satellite cloud cover (mean octas) June 1967-70

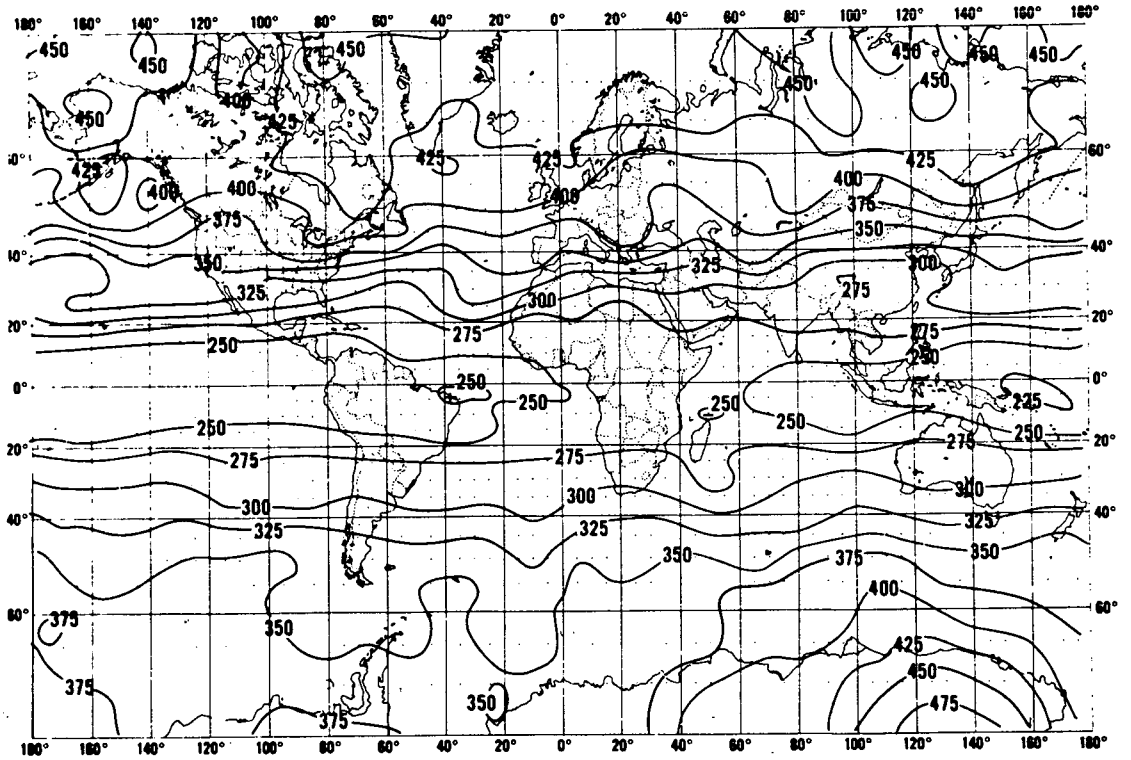

Figure 8a. Monthly mean ozone map (IRIS data) for April 1969

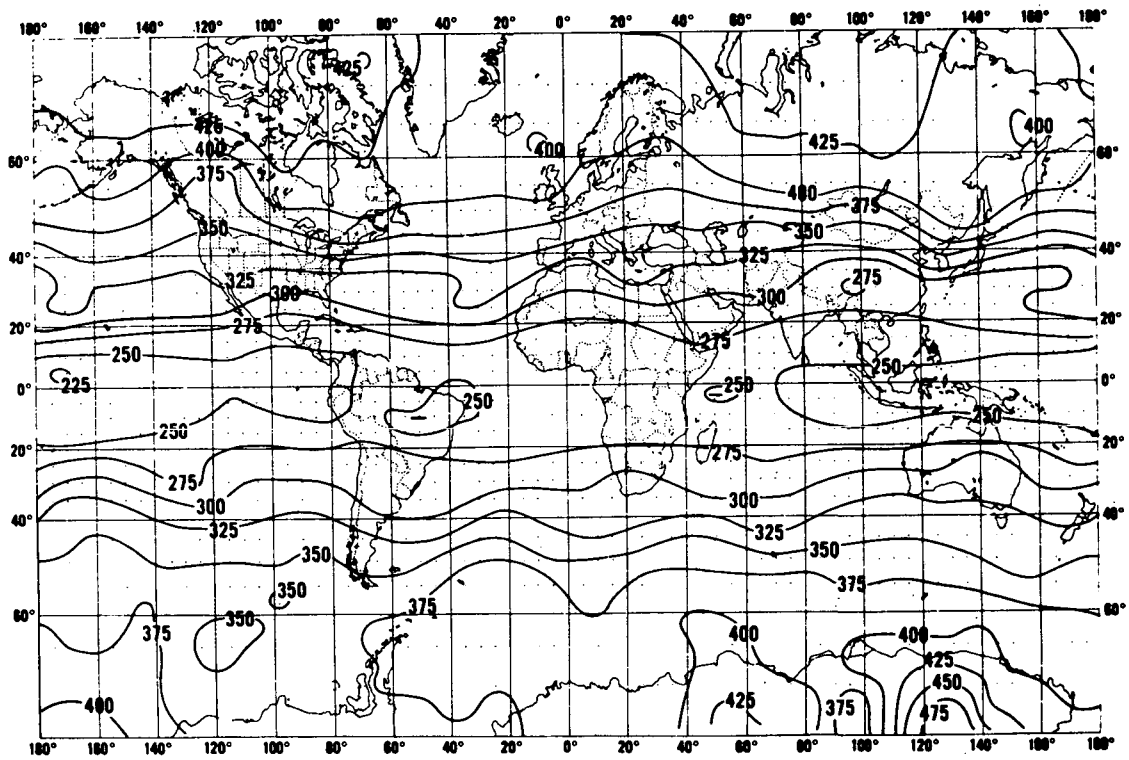

Figure 8b. Monthly mean ozone map (IRIS data) for May 1969

ozone maps also exhibit the same feature. IRIS total ozone map for April 23 (Figure 9), that for April 24 (Figure 1c) and the BUV total ozone map for June 21-28 (Figure 10), are instances in point.

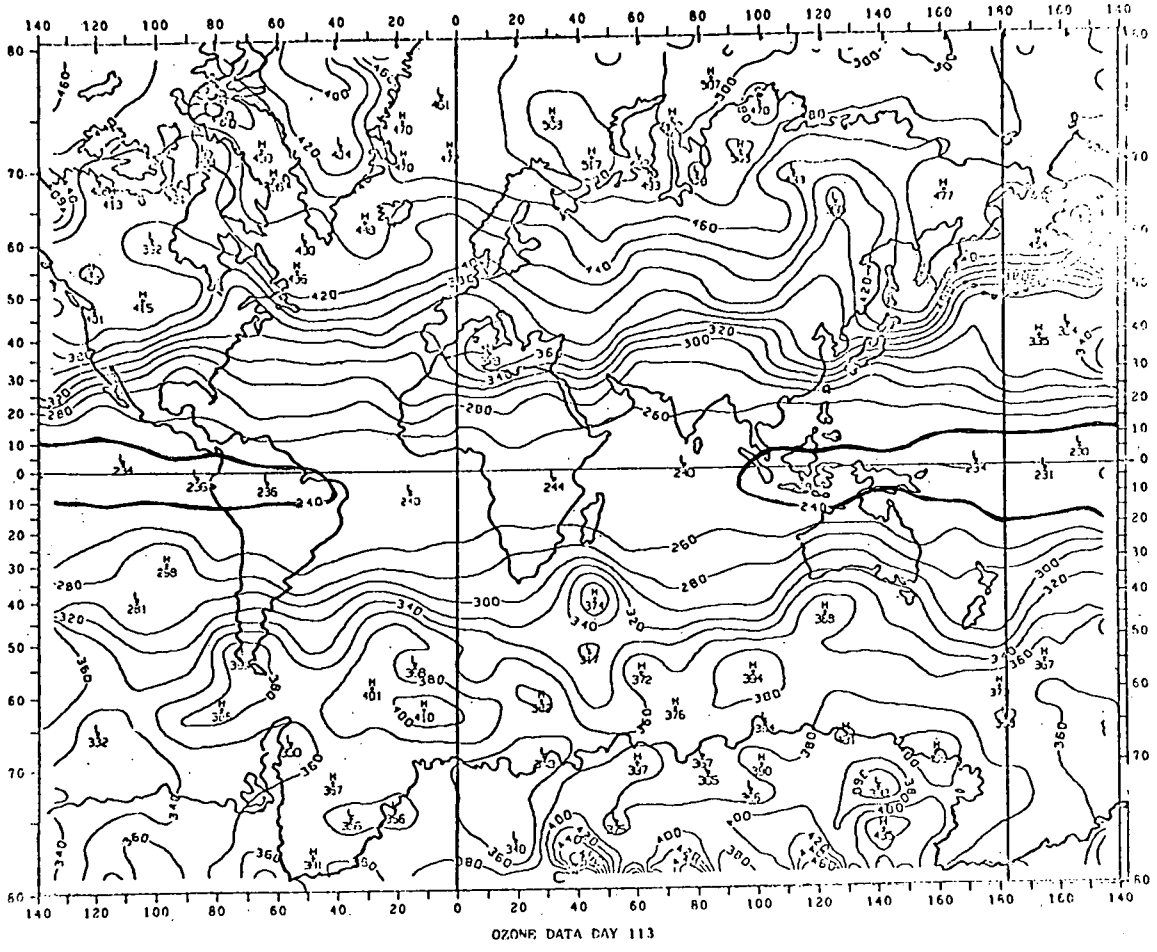

Figure 9. IRIS total ozone map of April 23, 1970

Evidently, there is a longitudinal inhomogeneity in the equatorial belt in cloud as well as in ozone distribution. One may consider what possible atmospheric circulations are consistent with this zonal asymmetry. It is well-known that during these months the extensive, and world's-highest plateau over Tibet

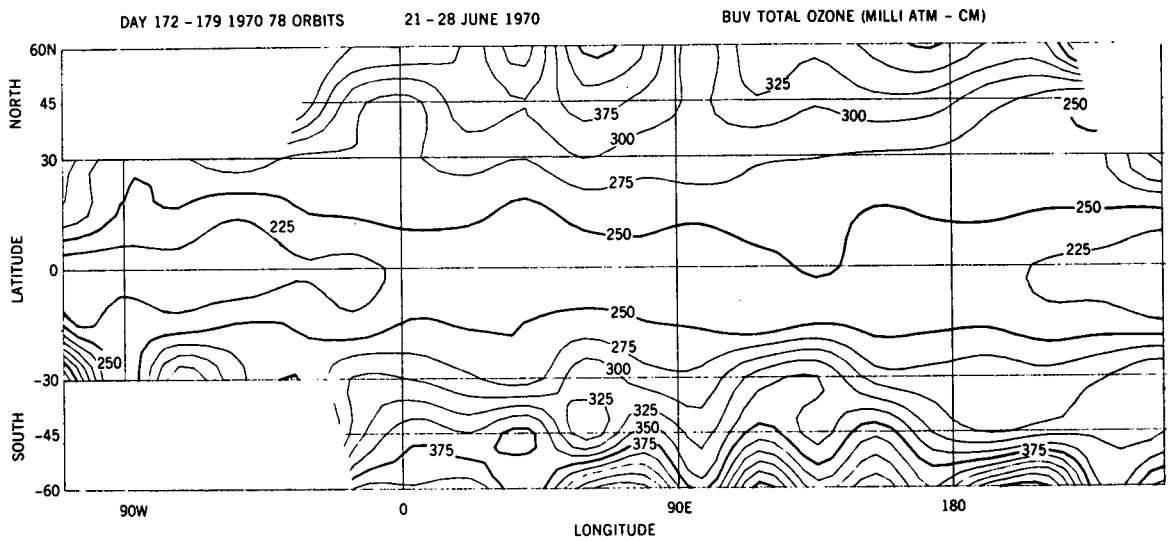

Figure 10. BUV total ozone map for June 21-28

(see map in Figure 11) is heated by the sun to the point where it becomes a major source of heat in the earth-atmospheric system. Koteswaram (unpublished) has indicated that a meridional circulation prevails with air rising over Tibet at about 30N and sinking close to the equator. This constitutes a reversed type of Hadley cell locally in that particular part of the globe. While this cell is thermally direct as in the usual Hadley circulation (the rising branch being at a relatively higher temperature than the descending branch with consequent generation of kinetic energy), the sense of the circulation is opposed to that of the normal Hadley cell in that the upper level flow here is southwards whereas it is northwards in the regular Hadley circulation. Owing to coriolis force the plane of the circulation has a NE-SW orientation, so that although air rises over Tibet (80-100E) the downward motion takes place in the Indian Ocean close to the African coast (40-60E). In other parts of the tropical belt, the traditional Hadley

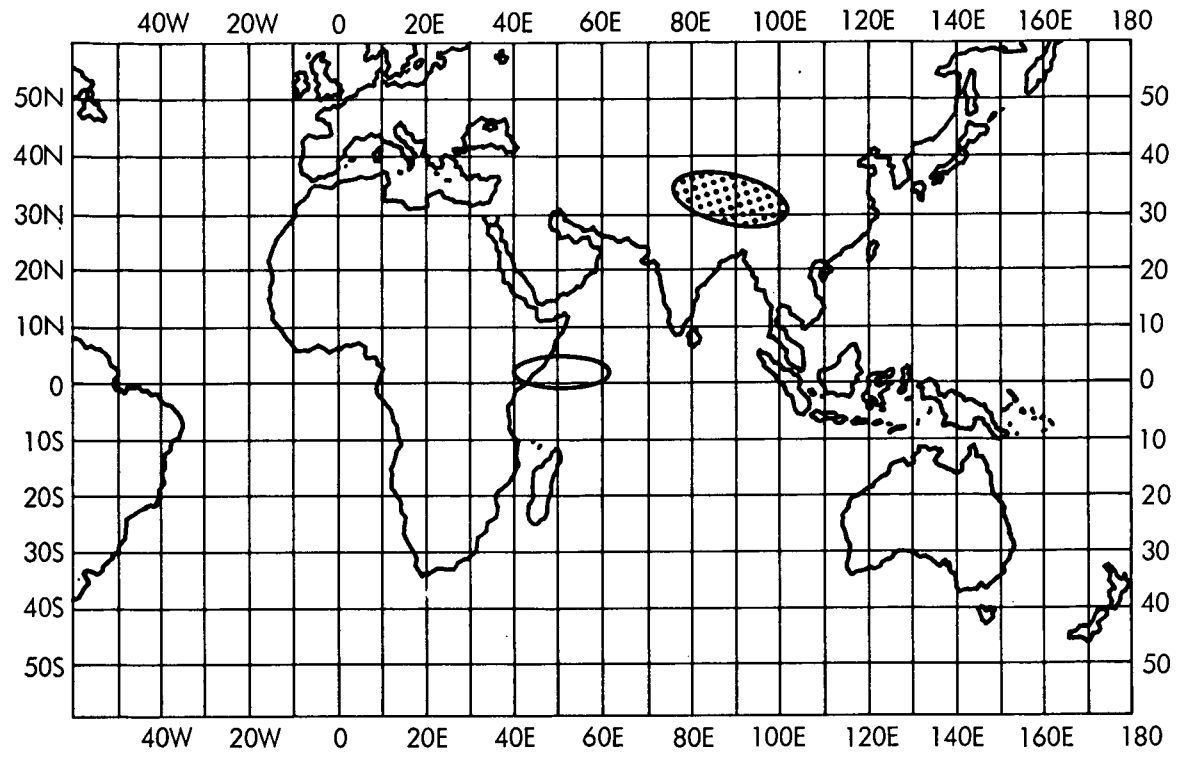

Figure 11. Map of the Indo-African area

type of circulation prevails with rising motion in the vicinity of the equator, flow towards North and East, and subsidence in sub-tropical latitudes. It has been suggested by some workers (e.g. Krishnamurti 1972) that the Mexican plateau which is lower and less extensive than the Tibetan plateau may produce a significant effect on the general circulation but definite evidence for this is lacking in the present study. A possible schematic circulation pattern consistent with the data examined (with the unconventional Hadley cell over the Indo-African region and the generally accepted type of Hadley circulation elsewhere) is presented in Figure 12. Let us consider the effect of such a circulation system on clouds and ozone. At those latitudes along the equator where there is

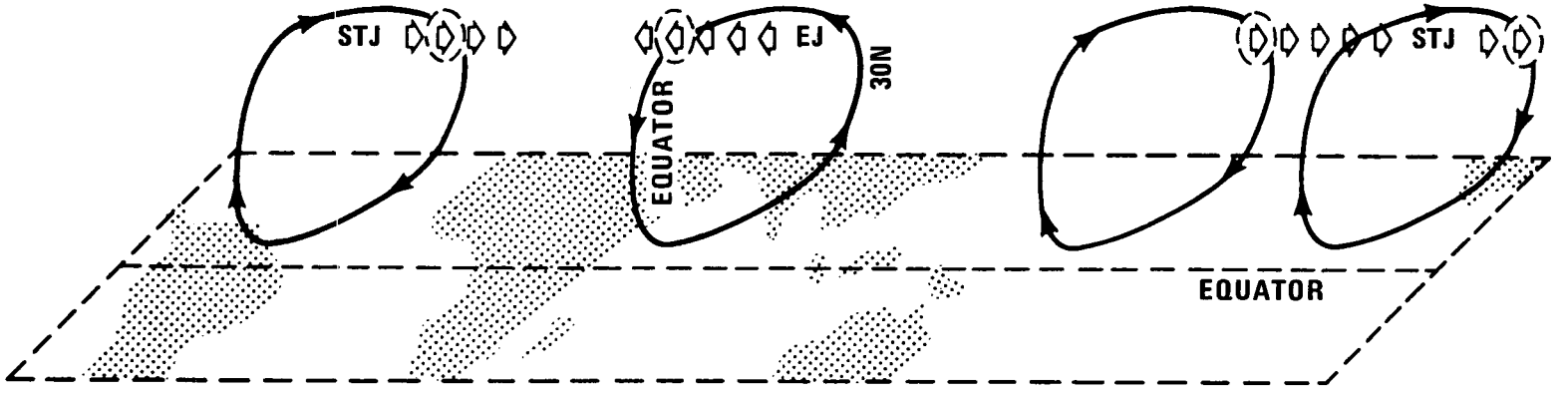

Figure 12. Reverse Hadley Cell over the Indo-African area with the regular Hadley circulation elsewhere. (STJ = Sub-Tropical Jet. EJ - Easterly Jet)

downward motion, as may be expected, the skies are relatively cloud-free. As for ozone, it is well established that there is no source of ozone of importance below the tropopause. The tropopause derives its main supply of ozone from the lower stratosphere of high latitudes (where ozone accumulates in winter) by the process of mixing, mostly in spring, along isentropic surfaces, through the tropopause break. The region round about 30N between 100 to 200 mb may thus be regarded as an ozone source region, so far as the lower atmosphere is concerned. Although ozone gets mixed in the troposphere by turbulence, the effect of a local reversed Hadley cell would be a preferential transfer of ozone from the source region at high levels around 30N to the zone where there is sinking air motion, i.e., 40-60E. It is possible that the observed consistently higher ozone in the Indo-African latitudes may be accounted for by this mechanism.

A comparison of the vertical distribution of ozone observed at Canal Zone and Leopoldville (extracted from Hesstvedt 1965 and presented in Figure 13) leads to the conclusion that the excess of ozone over Leopoldville is to be found in the troposphere (while between 23 and 28 km there appears to be a relative deficit). Furthermore, Griggs (1963) has reported on bubbler ozonesonde measurements over Nairobi, which reveal rather low ozone concentrations over the tropopause. These results do not favor an alternative mechanism (which one may be tempted to consider) invoking transfer of ozone into the lower stratosphere over the African continent.

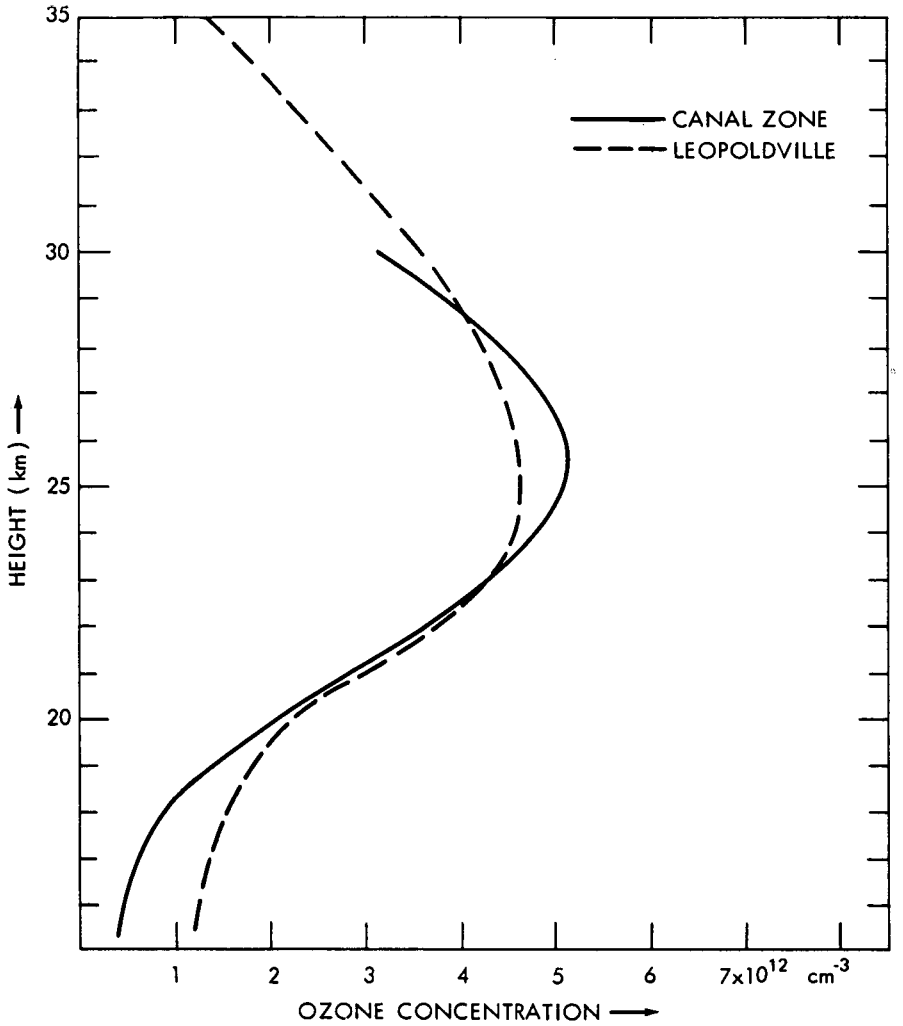

Figure 13. Vertical distributions of ozone observed over Canal Zone and Leopoldville (after Hesstvedt)

Sea-surface temperatures during May 4 — June 2, 1970, deduced from Nimbus 4 THIR data by Salomonson (unpublished) are presented in Figure 14. One may see a minimum temperature of 24°C close to the equator between 40E and 55E. The cause of this minimum is upwelling due to southwesterly surface winds along the Somali coast. The SW winds which occur over the area are consistent with a reversed Hadley cell. In the light of the correlation between warm

seas and upward air-motion, the low temperature sea-area is compatible with the atmospheric sink above.

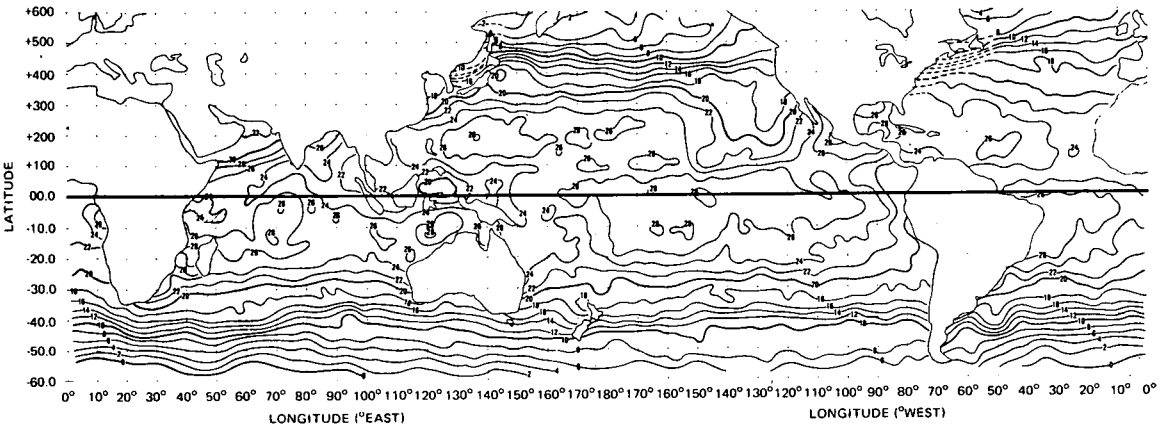

Figure 14. Sea-surface temperatures during May 4-June 2, 1970 deduced from Nimbus 4 THIR data

The transport of momentum by the reversed Hadley cell would be in the sense opposite to that by the conventional Hadley circulation. The axis of the sub-tropical westerly jet-stream is normally close to where the northward flow at upper levels in the general Hadley cell ends, yielding to downward motion. It is perhaps more than a coincidence that the axis of the easterly jet stream which is observed only in the Indo-African part of the tropics, is located nearly where the southward flow at high levels in the reversed Hadley cell inferred above, terminates (Figure 12).

The scheme put forward here is supported by some of the findings of Saha (1971) who from a number of considerations deduces a zonal type of circulation in the tropics with its descending limb at 45-55E. Saha's suggestion that the

ascent occurs over the eastern Indian Ocean does not, however, fit in with the cloud, ozone and ocean surface temperature data examined in this study. Also, Krishnamurti (1972), from a survey of global commercial aircraft reports, has arrived at a distribution of velocity potential at 200 mb, with a peak value in the tropics of 7×10^6 meter^2 sec^{-1} in the neighborhood of 20N 100E, the direction of the steepest gradient from this potential hill, along which the airstream runs, being southeastwards. There is thus broad agreement between this and the present results, although the location of the potential peak is slightly to the southeast of the Tibetan plateau at a place where it is difficult to think of an immediate physical reason for high-level divergence.

4. WINDS AND OZONE GRADIENTS

Prabhakara, Rodgers and Salomonson (1973) have demonstrated a high correlation between ozone amount and geopotential height, and deduced the geostrophic winds at 200 mb using total ozone as a quasi-stream function. Understandably, therefore, jet streams are associated with ozone gradients. During the course of the present investigation, this association was observed to be generally valid. Figure 15a presents the total ozone map of June 9, 1970, while Figure 15b reproduces the 200 mb (1200z) chart of the same day. Between 42N and 46N, 120E to 130E on that day the jet speed attains a maximum of 80-100 kt; in the same area the ozone gradient is strong reaching a maximum value of 16 Dobson units per degree latitude. Similarly between 36 and 45N, 180 to 130W, the jet again picks up speed to more than 80 kt and correspondingly the ozone

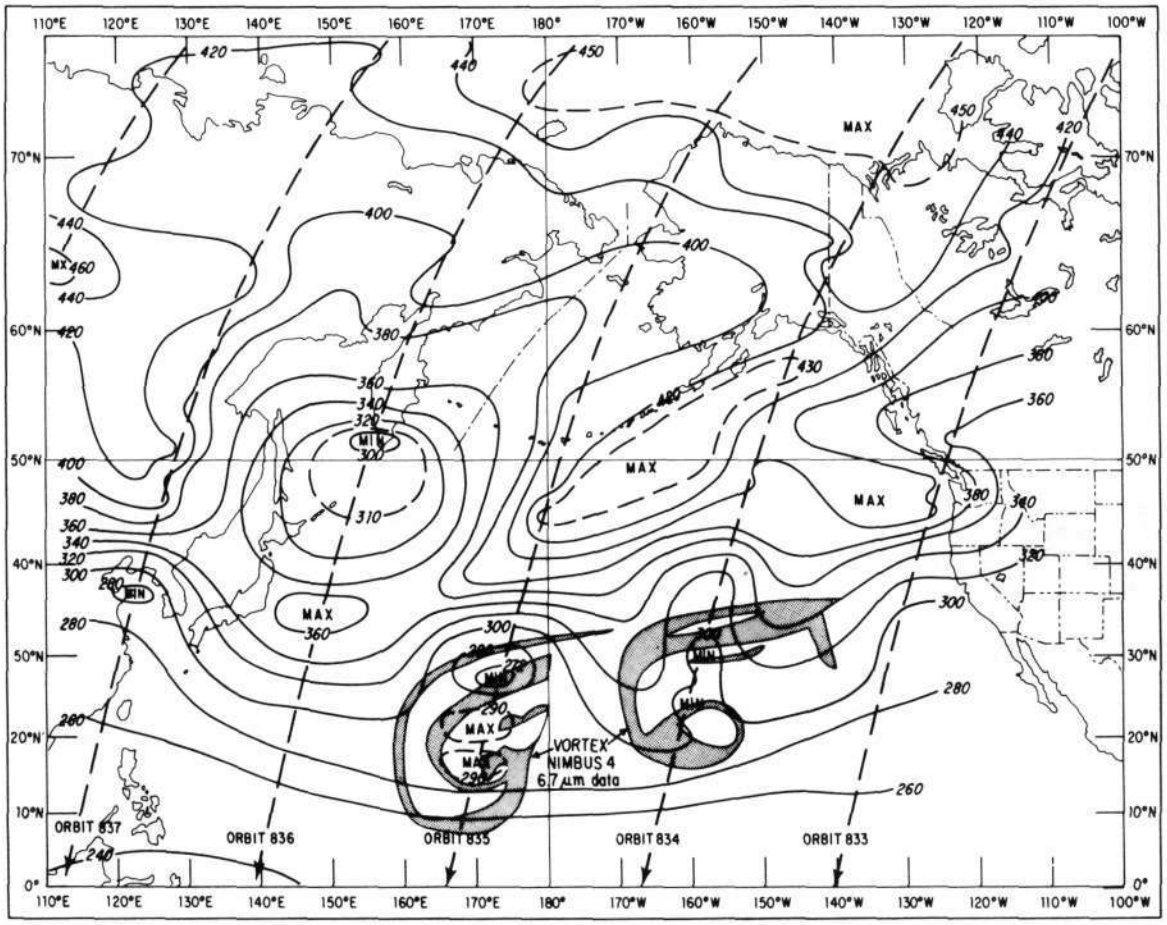

Figure 15a. Total ozone map for June 9, 1970

gradient in the region strengthens. Furthermore, the axis of the jet appears to be covered at intervals (as in earlier instances) with little cells of ozone maxima. These cells may be the result of clouds, or of eddies associated with the jet, or of a wave pattern along the jet axis. In any event, the ozone gradient as well as the cells of ozone maxima in the vicinity of the jet bear out earlier results.

5. CONCLUDING REMARKS

In this investigation, results from a number of satellite experiments enabled a composite study being made of several types of data such as cloud, ozone

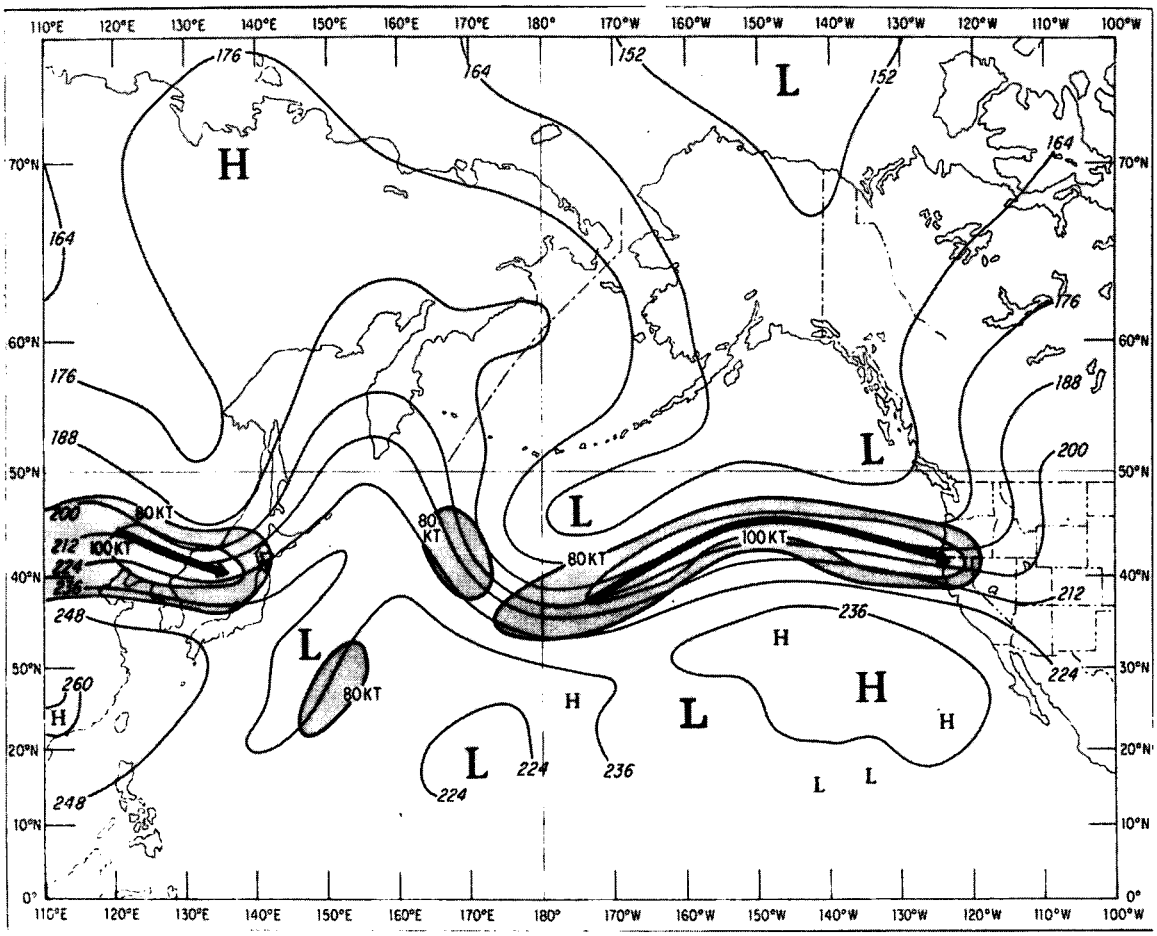

Figure 15b. 200 mb (1200z) chart of the same day

and sea-surface temperature. The main conclusions that may be drawn are:

1. (a) There is a close relationship between vortices in the troposphere and maxima in total ozone.

   (b) The enhancement in ozone associated with these vortices occurs predominantly in the lower stratosphere.

2. (a) The equatorial belt exhibits longitudinal inhomogeneity in respect of several meteorological parameters; it is marked by an area of

minimum cloudiness, comparatively high ozone and low sea-surface temperature in the Indo-African region.

(b) A possible meridional circulation consistent with this inhomogeneity is a reversed Hadley cell in summer locally over the Indo-African area.

3. The association of high level winds with ozone gradients and of jet streams with tiny cells of ozone maxima, is further substantiated.

It would be desirable to introduce a scanning device for ozone measuring equipment on spacecraft; from the resulting improved data coverage more exact conclusions could be drawn.

It is further suggested that a program may be undertaken (perhaps as a part of GARP) to determine the vertical velocity (w) in the African and Indian Ocean regions for verifying the reality of the reverse Hadley circulation. Probably the best procedure would be evaluation of w from the continuity equation, horizontal divergence from the earth's surface upwards being derived from winds measured by a close network of radar wind observing posts. Such data would be invaluable in understanding the general circulation.

ACKNOWLEDGEMENTS

Thanks are due to V. V. Salomonson for permitting the use of sea-surface temperature chart reproduced in Figure 14 and to L. J. Allison for supplying Figure 15.

During the period of this investigation, M. S. V. Rao was the recipient of a NRC-NASA Research Associateship.

REFERENCES

1. Hanel, R., Conrath, B., and Schlachman, B. "The Infrared Interferometer Spectrometer Experiment." Nimbus 4 User's Guide, Goddard Space Flight Center, Greenbelt, Md. (1970), 65-100

2. Heath, D., Krueger, A. J., and Mateer, C. "The Backscatter Ultraviolet Spectrometer Experiment." Nimbus 4 User's Guide, Goddard Space Flight Center, Greenbelt, Md. (1970) 149-169

3. Hesstvedt, E. "Ozone Distribution Over the Equator and its Dependence on Vertical Motions." Tellus, Vol. 17, No. 2 (1965) 177-178

4. Griggs, M. "Measurements of the Vertical Distribution of Atmospheric Ozone at Nairobi." Quarterly Journal of the Royal Meteorological Society, Vol. 89 (1963) 284-286

5. Koteswaram, P. (Unpublished) Indian Meteorological Service, New Delhi

6. Krishnamurti, T. N. "Observational Studies on Tropical General Circulation." Final Report to NSF Grant No. GA 17822, Department of Meteorology, Florida State University (1972)

7. McCulloch, A. W. "The Temperature-Humidity Infrared Radiometer Experiment." Nimbus 4 User's Guide, Goddard Space Flight Center, Greenbelt, Md. (1970), 25-64

8. Prabhakara, C., Conrath, B. J., Allison, L. J. and Steranka, J. "Seasonal and Geographical Variation of Atmospheric Ozone Derived from Nimbus 3." NASA Technical Note D 6443 (1971)

9. Prabhakara, C., Rodgers, E. B., and Salomonson, V. V. "Remote Sensing of Global Distribution of Total Ozone and the Inferred Upper Tropospheric Circulation from Nimbus IRIS Experiments." Pure and Applied Geophysics (1973)

10. Saha, K. R. "Cloud Distributions Over Equatorial Indian Ocean as Revealed by Satellites." Indian Journal of Meteorology and Geophysics, Vol. 22 (1971) 389-396

11. Salomonson, V. V. (Unpublished). Goddard Space Flight Center, Greenbelt, Md.

12. Werner, E. and Branchflower, G. A. "The Image Dissector Camera System." Nimbus 4 User's Guide, Goddard Space Flight Center, Greenbelt, Md. (1970) 11-24

* U. S. GOVERNMENT PRINTING OFFICE: 1972—735-966/540